

Automatically selecting a suitable integration scheme for systems of differential equations in neuron models.

Inga Blundell^{1,*}, Dimitri Plotnikov^{2,3}, Jochen Martin Eppler² and Abigail Morrison^{1,2,4}

¹*Institute of Neuroscience and Medicine (INM-6), Institute for Advanced Simulation (IAS-6), JARA BRAIN Institute I, Forschungszentrum Jülich, Jülich, Germany*

²*Simulation Lab Neuroscience, Institute for Advanced Simulation, JARA, Forschungszentrum Jülich, Jülich, Germany*

³*Chair of Software Engineering, Jülich Aachen Research Alliance (JARA), RWTH Aachen University, Aachen, Germany*

⁴*Institute of Cognitive Neuroscience, Faculty of Psychology, Ruhr-University Bochum, Bochum, Germany*

Correspondence*:
Inga Blundell
i.blundell@fz-juelich.de

1 ABSTRACT

2 On the level of the spiking activity, the
3 integrate-and-fire neuron is one of the most
4 commonly used descriptions of neural activ-
5 ity. A multitude of variants has been proposed
6 to cope with the huge diversity of behaviors
7 observed in biological nerve cells. The main
8 appeal of this class of model is that it can be
9 defined in terms of a hybrid model, where a
10 set of mathematical equations describes the
11 sub-threshold dynamics of the membrane po-
12 tential and the generation of action potentials
13 is often only added algorithmically without the
14 shape of spikes being part of the equations. In
15 contrast to more detailed biophysical models,
16 this simple description of neuron models allows
17 the routine simulation of large biological neu-
18 ronal networks on standard hardware widely
19 available in most laboratories these days.

20 The time evolution of the relevant state vari-
21 ables is usually defined by a small set of
22 ordinary differential equations (ODEs). A small

number of evolution schemes for the corre- 23
sponding systems of ODEs are commonly 24
used for many neuron models, and form the 25
basis of the neuron model implementations 26
built into commonly used simulators like Brian, 27
NEST and NEURON. 28

However, an often neglected problem is that 29
the implemented evolution schemes are only 30
rarely selected through a structured process 31
based on numerical criteria. This practice can- 32
not guarantee accurate and stable solutions for 33
the equations and the actual quality of the so- 34
lution depends largely on the parametrization 35
of the model. 36

In this article, we give an overview of typical 37
equations and state descriptions for the dynam- 38
ics of the relevant variables in integrate-and-fire 39
models. We then describe a formal mathemati- 40
cal process to automate the design or selection 41
of a suitable evolution scheme for this large 42
class of models. Finally, we present the refer- 43
ence implementation of our symbolic analysis 44
toolbox for ODEs that can guide modelers 45

46 during the implementation of custom neuron
47 models.

48 **Keywords:** integrate-and-fire neuron, model dynamics, numer-
49 ics, integration schemes, ODE, symbolic analysis

$$\frac{d}{dt}\mathbf{X} = \frac{d}{dt} \begin{pmatrix} V \\ x_1 \\ \vdots \\ x_n \end{pmatrix} (t) = \begin{pmatrix} R_0(\mathbf{X}) \\ R_1(\mathbf{X}) \\ \vdots \\ R_n(\mathbf{X}) \end{pmatrix}$$

1 INTRODUCTION

50 In common with all body cells, nerve cells (*neurons*)
51 are delimited by a bi-lipid layer (the *cell membrane*)
52 which is largely impermeable for ions and bigger
53 molecules. Active ion pumps and passive channels
54 embedded into the membrane allow the selective
55 passage of certain ions. Through these transporter
56 molecules, neurons maintain a gradient of different
57 ion types across the membrane, which leads to the
58 *membrane potential* (Kandel et al., 2013).

59 In the absence of input, the membrane potential
60 fluctuates around the *resting potential* E_L (typically
61 at around -70 mV). Excitatory input depolarizes
62 the membrane, driving the membrane potential
63 closer to zero, while inhibitory input hyperpolarizes
64 the neuron, driving the membrane potential away
65 from zero. If the membrane potential crosses the
66 *spiking threshold* θ (typically at around -55 mV),
67 the neuron fires an action potential (*spike*), which
68 is transmitted to all downstream (*postsynaptic*) neu-
69 rons, where it in turn elicits excursions of their
70 membrane potentials.

71 The basic integrate-and-fire model describes the
72 dynamics of the membrane potential in the fol-
73 lowing way: the time evolution of the membrane
74 potential V is governed by a differential equation
75 of the type

$$\frac{d}{dt}V(t) = R(V(t), \cdot) \quad (1)$$

76 where R can be a function of other variables
77 alongside V , whose time evolution is described by
78 another ordinary differential equation which can
79 again contain the membrane potential:

80 Once the membrane potential reaches its thresh-
81 old θ , a spike is fired and the membrane potential is
82 set back to E_L for a certain amount of time called
83 the *refractory period*. After this time the evolution
84 of Equation 1 starts again. An important simplifi-
85 cation in most models compared to biology is that
86 the exact course of the membrane potential during
87 the spike is either completely neglected or only con-
88 sidered partially. Threshold detection is typically
89 added algorithmically on top of the sub-threshold
90 dynamics.

91 The two most common variants of this type of
92 model are the *current-based* and the *conductance-*
93 *based* integrate-and-fire model. For the current-
94 based model we have the following general form of
95 the equation:

$$\begin{aligned} \frac{d}{dt}V(t) &= \frac{1}{\tau}(E_L - V(t)) \\ &+ \frac{1}{C}I(t) + F(V(t)). \end{aligned} \quad (2)$$

96 Here C is the *membrane capacitance*, τ the *mem-*
97 *brane time constant* and I the *input current* to the
98 neuron. If we assume that spikes are constrained
99 to a fixed temporal grid, $I(t)$ represents the sum of
100 the currents elicited by all incoming spikes at all
101 grid points for times smaller than t , plus a piece-
102 wise constant function I_{ext} that models additional
103 external input. F , in contrast to the first part of the
104 right-hand-side of Equation 2, is some non-linear
105 function of V that may also be zero.

106 For the conductance-based integrate-and-fire
107 model we have:

$$\frac{d}{dt}V(t) = \frac{1}{\tau}(E_L - V(t)) + \frac{1}{C}G(t)(V(t) - E) + F(V(t)). \quad (3)$$

108 G has the same form as I but models a con-
 109 ductance rather than a current. E is the *reversal*
 110 *potential* at which there is no net flow of ions
 111 from one side of the membrane to the other (for
 112 details see Kandel et al., 2013). Equation 3 will usu-
 113 ally contain several summands $\frac{1}{C}G_i(t)(V(t) - E_i)$
 114 for differing G_i and corresponding E_i , e.g. for in-
 115 hibitory and excitatory synaptic conductance. For
 116 simplicity we assume only one summand. The
 117 differential equations for both the current- and
 118 conductance-based models are linear when $F \equiv 0$.
 119 For the current-based model this means that Equa-
 120 tion 2 is a linear *constant coefficient* differential
 121 equation.

122 An example of a neuron model described by a
 123 system of differential equations, where $F \neq 0$ is
 124 the *adaptive exponential integrate-and-fire model*:

$$\begin{aligned} \frac{d}{dt}V(t) &= \frac{1}{\tau}(E_L - V(t)) \\ &+ \frac{1}{C}G(t)(V(t) - E) \\ &+ g \cdot \delta \cdot \exp\left(\frac{V(t) - V_T}{\delta}\right) - w(t) \\ \frac{d}{dt}w(t) &= \frac{c}{\tau_w}(V(t) - E_L) \end{aligned}$$

125 For the biophysical meaning of the variables V_T ,
 126 δ , g , c , τ_w and w see the original publication by
 127 Brette and Gerstner (2005).

128 Current-based neuron models with $F \neq 0$ are un-
 129 usual because models from this category are chosen
 130 primarily for their simplicity, while conductance-
 131 based neuron models are believed to describe neu-
 132 ron activity in the brain more accurately, albeit at
 133 the cost of more complex differential equations.

It should be noted here that although some neuron
 models are not explicitly referred to or described as
current-based or *conductance-based* models in the
 literature their time evolution can still be expressed
 by differential equations of the mathematical forms
 shown in Equations 2 and 3.

The choice of an appropriate solver for a given
 equation is a non-trivial task, as it requires deep
 knowledge of ordinary differential equations and
 numerics to assess the type of differential equation
 and construct an appropriate numeric solver. This
 choice depends not only on the form of the dif-
 ferential equation but also on the magnitude of the
 occurring parameters. For example, Rotter and Dies-
 mann (1999) demonstrated that for neuron models
 that can be expressed as time-invariant linear sys-
 tems, the analytical solution to the evolution of the
 dynamics from one time step to the next can be
 achieved by a matrix multiplication. If applicable,
 this kind of solution is to be preferred, as it is both
 exact and computationally efficient.

However, this approach leaves two key steps up
 to the modeller: firstly, analyzing the dynamics to
 discern what category of dynamical system it is; sec-
 ondly, having performed this analysis, to construct
 the appropriate solver, e.g. the terms of the propa-
 gator matrix for such neurons that can be solved in
 this way (Rotter and Diesmann, 1999) or the config-
 uration of an implicit or explicit numeric solver for
 all other neuron models. As these steps can be quite
 challenging to many modellers, it would be of great
 use to have a framework capable of automatically
 performing this analysis and solver construction.

In Section 2 we therefore first derive compact
 canonical representations of the equations and their
 parts that allow an efficient implementation on a
 computer system, and then show that the distinc-
 tion between current- and conductance-based, linear
 and non-linear, stiff and non-stiff systems of differ-
 ential equations is important for automatizing the
 construction or selection of an optimal evolution
 scheme.

Our reference implementation follows the mathe-
 matical observations and is described in Section 3.

178 Section 4 demonstrates our application of the frame-
 179 work to some commonly used models in computa-
 180 tional neuroscience and explains the integration of
 181 the framework into the NEST Modeling Language
 182 (NESTML; Plotnikov et al., 2016). We close with
 183 a presentation of related work in Section 5 and a
 184 discussion and outlook in Section 6, where we sum-
 185 marize possible extensions and further applications
 186 of our system.

2 MATERIALS AND METHODS

187 As already pointed out in the previous section,
 188 systems of differential equations describing the
 189 dynamics in neuron models can be divided into
 190 *current-based* and *conductance-based* systems. Ad-
 191 ditional distinguishing properties are whether the
 192 systems are *linear* or *non-linear*, *stiff* or *non-stiff*.
 193 We will now describe how these properties influence
 194 the choice of an appropriate solver.

195 For the current-based integrate-and-fire neuron
 196 with $F \equiv 0$, we have a first order constant coeffi-
 197 cient linear differential equation where I typically
 198 satisfies a homogeneous linear differential equation
 199 of some order $n \in \mathbb{N}$. Any such ODE or system of
 200 ODEs can be solved analytically and efficiently as
 201 we will show in Section 2.1.

202 When evolving systems of ODEs for conductance-
 203 based linear or non-linear ODEs, it is necessary
 204 to use a numeric integration scheme. Depending
 205 on the system at hand, it is advisable to choose
 206 either an implicit or an explicit stepping function
 207 (Section 2.2).

208 2.1 Solving linear constant coefficient 209 ODEs analytically

210 For simplicity we will assume E_L in Equation 2
 211 to be zero or to be included in one of the other
 212 terms of the right hand side. As shown by Rotter
 213 and Diesmann (1999), if $V : \mathbb{R} \rightarrow \mathbb{R}$ satisfies the
 214 first order constant coefficient linear differential
 215 equation

$$\frac{d}{dt}V(t) = -\frac{1}{\tau}V(t) + \frac{1}{C}I(t) \quad (4)$$

with initial value $V(0) = V_0$, for a function $I : \mathbb{R}^+$
 $\mathbb{R}^+ \rightarrow \mathbb{R}$ and constants C (the capacitance of the
 membrane) and τ (the membrane time constant),
 and if I satisfies

$$\left(\frac{d}{dt}\right)^n I = \sum_{i=0}^{n-1} a_i \left(\frac{d}{dt}\right)^i I \quad (5)$$

for some $n \in \mathbb{N}$ and a sequence $(a_i)_{i \in \mathbb{N}} \subset \mathbb{R}$, an
 analytical solver can be constructed in the form of
 a propagator matrix.

Here, we show how to evaluate the dynamics to
 discern whether V and I do indeed satisfy the condi-
 tions stated above, and how to derive the evolu-
 tions scheme for V accordingly. First, we verify that
 the first order differential equation, $\frac{d}{dt}V = r(V)$,
 for a right hand side $r : \mathbb{R} \times \mathbb{R}^+ \rightarrow \mathbb{R}$, is in-
 deed linear with a constant coefficient, i.e. that
 $\left(\frac{d}{dV}\right)^2 r(V) = 0$ and $\left(\frac{d}{dV}\right) r(V)(t)$ is constant. Sec-
 ond we methodically determine whether I satisfies
 a linear differential equation of some order n , i.e.
 we check whether

$$\frac{d}{dt}I = a_0 I \quad (6)$$

for some $a_0 \in \mathbb{R}$ by solving for a_0 . If no such a_0
 exists we check whether

$$\left(\frac{d}{dt}\right)^2 I = a_0 I + a_1 \frac{d}{dt}I \quad (7)$$

for some $a_0, a_1 \in \mathbb{R}$ using the following proce-
 dure: we assume that a_0, a_1 exist such that (7) is
 satisfied. Then we have for some $t_1, t_2 \in \mathbb{R}$ (for
 example $t_1 = 1, t_2 = 2$):

$$\mathbf{X}(t_1, t_2) := \begin{pmatrix} I(t_1) & \frac{d}{dt}I(t_1) \\ I(t_2) & \frac{d}{dt}I(t_2) \end{pmatrix},$$

$$\mathbf{X}(t_1, t_2) \cdot \begin{pmatrix} a_0 \\ a_1 \end{pmatrix} = \begin{pmatrix} \left(\frac{d}{dt}\right)^2 I(t_1) \\ \left(\frac{d}{dt}\right)^2 I(t_2) \end{pmatrix}$$

If $\det(\mathbf{X}(t_1, t_2)) \neq 0$ we therefore know that

$$\begin{pmatrix} a_0 \\ a_1 \end{pmatrix} = \mathbf{X}^{-1}(t_1, t_2) \cdot \begin{pmatrix} \left(\frac{d}{dt}\right)^2 I(t_1) \\ \left(\frac{d}{dt}\right)^2 I(t_2) \end{pmatrix}.$$

241 Under the assumption that (7) is satisfied and that
 242 $\det(\mathbf{X}(t_1, t_2)) \neq 0$ this gives us a_0 and a_1 . If our
 243 second assumption is not satisfied we can easily
 244 chose t_1 and t_2 so that it is. We can now determine
 245 whether the first assumption is correct by inserting
 246 the calculated values for a_0 and a_1 and checking if
 247 the following equation is true:

$$\left(\frac{d}{dt}\right)^2 I - a_0 I - a_1 \frac{d}{dt} I = 0 \quad (8)$$

248 Now, if such a_0 and a_1 exist, they are unique,
 249 as I and $\frac{d}{dt} I$ are linearly independent, since there
 250 was no $a_0 \in \mathbb{R}$ such that (6) was satisfied. If a_0
 251 and a_1 do not satisfy (8), we check methodically
 252 if constants $(a_i)_{i \in \mathbb{N}} \subset \mathbb{R}$ exist, for which (5) is
 253 satisfied for $n = 3, 4, \dots$. Again we assume that
 254 $a_0, \dots, a_n \in \mathbb{R}$ exist such that (5) is satisfied. Then
 255 we have for $t = (t_1, \dots, t_n) \in \mathbb{R}^n$ (for example
 256 $t_1 = 1, \dots, t_n = n$):

$$\mathbf{X}(t) := \begin{pmatrix} I(t_1) & \dots & \left(\frac{d}{dt}\right)^{n-1} I(t_1) \\ \vdots & \ddots & \vdots \\ I(t_n) & \dots & \left(\frac{d}{dt}\right)^{n-1} I(t_n) \end{pmatrix}, \quad (9)$$

$$\mathbf{X}(t) \cdot \begin{pmatrix} a_0 \\ \vdots \\ a_{n-1} \end{pmatrix} = \begin{pmatrix} \left(\frac{d}{dt}\right)^n I(t_1) \\ \vdots \\ \left(\frac{d}{dt}\right)^n I(t_n) \end{pmatrix}. \quad (10)$$

257 If $\det(\mathbf{X}(t)) \neq 0$ we get

$$\begin{pmatrix} a_0 \\ \vdots \\ a_{n-1} \end{pmatrix} = \mathbf{X}^{-1}(t) \cdot \begin{pmatrix} \left(\frac{d}{dt}\right)^n I(t_1) \\ \vdots \\ \left(\frac{d}{dt}\right)^n I(t_n) \end{pmatrix}. \quad (11)$$

Again, if $\det(\mathbf{X}(t)) = 0$ we simply use another t ,
 for example $t = (t_1 + 1, \dots, t_n + 1)$. Then we obtain
 the values of a_0, \dots, a_n under the assumption that
 (5) is satisfied for order n . We check whether the
 assumption in (5) is true by symbolically evaluating
 whether

$$\left(\frac{d}{dt}\right)^n I - \sum_{i=0}^{n-1} a_i \left(\frac{d}{dt}\right)^i I = 0.$$

If (5) is not satisfied we go on to check

$$\left(\frac{d}{dt}\right)^{n+1} I = \sum_{i=0}^n a_i \left(\frac{d}{dt}\right)^i I$$

for some a_0, \dots, a_{n+1} , and so on. This way, for
 every I that satisfies (5) for order n we can deter-
 mine the factors a_0, \dots, a_n . Then we can rephrase
 (4) as the *homogeneous* differential equation

$$\frac{d}{dt} \mathbf{y}(t) = \mathbf{A} \mathbf{y}(t) \quad (12)$$

with initial values $\mathbf{y}(0) = \mathbf{y}_0$, $\mathbf{y} =$
 $\left(\frac{d^{n-1}}{dt^{n-1}} I, \frac{d^{n-2}}{dt^{n-2}} I, \dots, I, V\right)$ and

$$\mathbf{A} = \begin{pmatrix} a_{n-1} & a_{n-2} & \dots & \dots & a_0 & 0 \\ 1 & 0 & \dots & 0 & 0 & 0 \\ 0 & \ddots & \ddots & \vdots & \vdots & \vdots \\ \vdots & \ddots & \ddots & 0 & 0 & 0 \\ 0 & 0 & \ddots & 1 & 0 & 0 \\ 0 & 0 & \dots & 0 & \frac{1}{C} & -\frac{1}{\tau} \end{pmatrix} \quad (13)$$

Thus for $n = 1$ we have

$$\mathbf{A} = \begin{pmatrix} a_0 & 0 \\ \frac{1}{C} & -\frac{1}{\tau} \end{pmatrix}$$

and for $n = 2$ we have

$$\mathbf{A} = \begin{pmatrix} a_1 & a_0 & 0 \\ 1 & 0 & 0 \\ 0 & \frac{1}{C} & -\frac{1}{\tau} \end{pmatrix}$$

273 As it can be both more convenient and computa-
 274 tionally more efficient when \mathbf{A} is a *lower triangular*
 275 matrix we give an alternative choice of \mathbf{A} and \mathbf{y} ,
 276 where \mathbf{A} is a triangular matrix:

$$\mathbf{A} = \begin{pmatrix} a_1 + x & 0 & 0 \\ 1 & -x & 0 \\ 0 & \frac{1}{C} & -\frac{1}{\tau} \end{pmatrix} \quad (14)$$

277 where

$$x = -\frac{a_1}{2} + \sqrt{\frac{a_1^2}{4} + a_0} \quad (15)$$

278 and

$$\mathbf{y} = \left(\frac{d}{dt} I + xI, I, V \right). \quad (16)$$

279 Then we can determine the solution \mathbf{y} at $t \in \mathbb{R}^+$
 280 using the matrix exponential:

$$\mathbf{y}(t) = e^{\mathbf{A}t} \mathbf{y}_0 \quad (17)$$

281 We can rephrase this to obtain an incremental for-
 282 mulation which allows the evolution of the system
 283 by a single calculation of $e^{\mathbf{A}h}$ for a fixed step size
 284 $h \in \mathbb{R}^+$:

$$\mathbf{y}(t+h) = e^{\mathbf{A}(t+h)} \cdot \mathbf{y}_0 = e^{\mathbf{A}h} \cdot \mathbf{y}_t.$$

285 It is important to note here that the exact inte-
 286 gration of (2) depends on the exact calculation of
 287 $e^{\mathbf{A}h}$. Let $I(t)$ be the sum of currents elicited by all
 288 incoming spikes at all grid points for times $t_i \leq t$,

$$I(t) = \sum_{i \in \mathbb{N}, t_i \leq t} \sum_{k \in S_{t_i}} I_k(t),$$

289 where $I_k(t) = \hat{v}_k \iota(t - t_i)$, for $t \in \mathbb{R}^+$. \hat{v}_k
 290 is the *synaptic weight* of synapse k and ι satis-
 291 fies the differential equation (5) on \mathbb{R}^+ for some
 292 constants $(a_i)_{i \in \mathbb{N}} \subset \mathbb{R}$ and some $n \in \mathbb{N}$. Then
 293 I satisfies the differential equation (5) on $\mathbb{R}^+ \setminus$

$\{t_1, \dots, t_k\}$. Therefore we can consider I as the
 294 solution of the differential equation (5) on the inter-
 295 vals $(0, t_1), (t_1, t_2), \dots$ with suitable initial values.
 296 For $t \in (t_{i-1}, t_i)$ we can calculate

$$\mathbf{y}(t) = e^{\mathbf{A}(t-t_{i-1})} \mathbf{y}_{t_{i-1}}.$$

At time t_i , for $i \in \mathbb{N}$, the differential equation
 298 (5) is not satisfied because ι does not satisfy the
 299 equation at $t = 0$, but we get $I(t_i)$ by continuous
 300 continuation to the boundary of the interval (t, t_i) .
 301 The derivatives of I contained in \mathbf{y} must be up-
 302 dated by initial values of additional spikes at time
 303 t_i , meaning for $\mathbf{P}(h) = e^{\mathbf{A}h}$

$$\mathbf{y}(t_i) = \mathbf{P}(h) \mathbf{y}(t_{i-1}) + \mathbf{x}_{t_i},$$

where

$$\mathbf{x}_{t_i} = \mathbf{T} \begin{pmatrix} \left(\frac{d}{dt} \right)^n \iota(0) \\ \vdots \\ \frac{d}{dt} \iota(0) \\ 0 \\ 0 \end{pmatrix} \sum_{k \in S_{t_i+h}} \hat{v}_k.$$

Here $\mathbf{T} \in \mathbb{R}^{n+1} \times \mathbb{R}^{n+1}$ is such that

$$\mathbf{y} = \mathbf{T} \begin{pmatrix} \left(\frac{d}{dt} \right)^{n-1} I \\ \vdots \\ I \\ V \end{pmatrix}$$

\mathbf{T} is the identity matrix when \mathbf{y} is chosen as the
 307 vector of derivatives as in Equation 12 and Equa-
 308 tion 13 but it may well be non-trivial, e.g. when \mathbf{y}
 309 is chosen as in Equation 16.

Now we know an analytical and efficient way
 311 to evolve any linear constant coefficient ODE con-
 312 taining the convolution of the solution of a linear
 313 homogeneous ODE and a weighted spike train.

315 2.1.1 Adding a constant external input
316 current

317 A common requirement in neuroscientific mod-
318 eling is to add a bias current to neurons. We will
319 now show how to solve the differential equation
320 when we have an additional constant external input
321 current I_E :

$$\begin{aligned}\frac{d}{dt}V &= \frac{d}{dt}(V_1 + V_2) = -\frac{V_1(t) + V_2(t)}{\tau} \\ &+ \frac{1}{C}(I(t) + I_E) \\ &= \frac{V(t)}{\tau} + \frac{1}{C}I(t) + \frac{I_E}{C}.\end{aligned}$$

and for $\mathbf{P} := \mathbf{P}(h) = e^{\mathbf{A}h}$ the following holds 328

$$\frac{d}{dt}V(t) = -\frac{V(t)}{\tau} + \frac{1}{C}(I(t) + I_E), \quad V(0) = V_0$$

322 As shown above, we can solve

$$\begin{aligned}V(t+h) &= \mathbf{P}_{n+1,1}\mathbf{y}_1(t) + \dots \\ &+ \mathbf{P}_{n+1,n+1}V_1(t) + V_2(t)e^{-h/\tau} \\ &+ \frac{I_E}{C}(1 - e^{-h/\tau}).\end{aligned}$$

$$\frac{d}{dt}V_1 = -\frac{V_1(t)}{\tau} + \frac{I(t)}{C}, \quad V_1(0) = V_{10}. \quad (18)$$

323 Consider the following differential equation,

$$\frac{d}{dt}V_2 = -\frac{V_2(t)}{\tau} + \frac{I_E}{C}, \quad V_2(0) = V_{20}, \quad (19)$$

324 where τ, C and I_E are constants. By *variation of*
325 *constants* (Walter, 2000) we have a solution of (19):

$$\begin{aligned}V_2(t) &= \left(\frac{I_E\tau}{C}e^{t/\tau} + V_{20} \right) e^{-t/\tau} \\ &= \frac{I_E\tau}{C} + V_{20}e^{-t/\tau},\end{aligned}$$

$$\begin{aligned}V_2(t+h) &= \frac{I_E\tau}{C} + V_{20}e^{-t/\tau}e^{-h/\tau} \\ &= V_2(t)e^{-h/\tau} + \frac{I_E\tau}{C}(1 - e^{-h/\tau}).\end{aligned}$$

326 Now we know solutions V_1 and V_2 of (18) and
327 (19). Therefore $V := V_1 + V_2$ solves

As the last column a in \mathbf{A} has only one entry 329
 $a_{n+1} = \frac{-1}{\tau}$ and $\mathbf{P} = e^{\mathbf{A}h} = \sum_{k=0}^{\infty} \frac{(\mathbf{A}h)^k}{k!}$, 330

$$\begin{aligned}\mathbf{P}_{n+1,n+1} &= \left(\sum_{k=0}^{\infty} \frac{(\mathbf{A}h)^k}{k!} \right)_{n+1,n+1} \\ &= \sum_{k=0}^{\infty} \frac{\left(\frac{-h}{\tau}\right)^k}{k!} = e^{-h/\tau}.\end{aligned}$$

We get: 331

$$\begin{aligned}V(t+h) &= \mathbf{P}_{n+1,1}\mathbf{y}_1(t) + \dots \\ &+ \mathbf{P}_{n+1,n}\mathbf{y}_n(t) \\ &+ V(t)e^{-h/\tau} + \frac{I_E\tau}{C}(1 - e^{-h/\tau}).\end{aligned}$$

This method is also applicable when we have 332
a piece-wise constant function \hat{y}_0 instead of a 333
constant I_E : 334

$$\frac{d}{dt}V_2 = -\frac{V_2(t)}{\tau} + \frac{\hat{y}_0}{C}, \quad V_2(0) = V_{20}.$$

335 where for all $i \in \mathbb{N}$ there is a $c_i \in \mathbb{R}$ such that
 336 $\hat{y}_0(t) = c_i$ for all $t \in [t_i, t_i + h)$. We rephrase the
 337 problem as:

$$\frac{d}{dt}V_{2_i} = -\frac{V_{2_i}(t)}{\tau} + \frac{c_i}{C}, \quad V_{2_i}(0) = V_{2_{i_0}}$$

338 on $t \in [t_i, t_i + h)$ for all $i \in \mathbb{N}$ and get

$$V_2(t_i) = \frac{c_i\tau}{C} + V_2(t_{i-1})e^{-h/\tau}$$

339 and

$$V(t_i) = V(t_{i-1})e^{-h/\tau} + \frac{c_i\tau}{C}(1 - e^{-h/\tau}).$$

340 Now we have an exact description for how to
 341 handle the evolution of linear constant coefficient
 342 ODEs containing the convolution of the solution of
 343 a linear homogeneous ODE and a weighted spike
 344 train with an additional constant external input, that
 345 is still analytical and efficient.

346 2.1.2 Handling sums

347 The approximation of postsynaptic currents ob-
 348 served in real brain experiments is sometimes
 349 best modeled by different functions for different
 350 synapses. We can handle the case when I is the sum
 351 of functions I_1, I_2 which satisfy a homogeneous
 352 differential equation of arbitrary order m and n in
 353 the following way. As seen above if V_1 is a solution
 354 of

$$\frac{d}{dt}V_1(t) = -\frac{V_1(t)}{\tau} + \frac{1}{C}I_1(t)$$

355 and V_2 is a solution of

$$\frac{d}{dt}V_2(t) = -\frac{V_2(t)}{\tau} + \frac{1}{C}I_2(t)$$

356 then $V = V_1 + V_2$ is a solution of

$$\frac{d}{dt}V(t) = -\frac{V(t)}{\tau} + \frac{1}{C}(I_1(t) + I_2(t)).$$

If, furthermore, I_1 satisfies (5) for $n \in \mathbb{N}$ 357

$$V_1(t+h) = \mathbf{P}_{n+1,1}^1 \mathbf{y}_1(t) + \dots \\ + \mathbf{P}_{n+1,n}^1 \mathbf{y}_n(t) + V_1(t)e^{-h/\tau}.$$

where \mathbf{P}^1 is the corresponding propagator matrix 358
 and I_2 satisfies (5) for some $m \in \mathbb{N}$ 359

$$V_2(t+h) = \mathbf{P}_{m+1,1}^2 \mathbf{y}_1(t) + \dots \\ + \mathbf{P}_{m+1,m}^2 \mathbf{y}_m(t) + V_2(t)e^{-h/\tau}$$

where \mathbf{P}^2 is the corresponding propagator matrix, 360
 then 361

$$V(t+h) = \mathbf{P}_{n+1,1}^1 \mathbf{y}_1(t) + \dots \\ + \mathbf{P}_{n+1,n}^1 \mathbf{y}_n(t) \\ + \mathbf{P}_{m+1,1}^2 \mathbf{y}_1(t) + \dots \\ + \mathbf{P}_{m+1,m}^2 \mathbf{y}_m(t) + V(t)e^{-h/\tau}.$$

Therefore we just need to compute two propagator 362
 matrices to handle the sum. 363

364 2.2 Choice of a suitable numeric 364 365 integration scheme 365

Explicit methods for solving differential equations 366
 are methods that only use already known values 367
 of the function at earlier grid points to determine 368
 the value at the next grid point. The efficiency 369
 and accuracy of explicit methods is typically suffi-370
 cient for systems of ODEs used to model neuronal 371
 behavior. Popular examples of such methods are 372
 the explicit 4th order classical Runge-Kutta or the 373
 explicit embedded Runge-Kutta-Fehlberg method 374
 (Dahmen and Reusken, 2005) for the approximative 375

376 solution of ODEs. Most neuron model implementa- 418
 377 tions currently use explicit stepping algorithms 419
 378 and still achieve satisfactory results in terms of ac- 420
 379 curacy and simulation time (Morrison et al., 2007; 421
 380 Hanuschkin et al., 2010). However, some published 422
 381 models involve possibly *stiff* differential equations
 382 (e.g. Brette and Gerstner, 2005), which potentially
 383 require a different class of solvers.

384 Lambert (1992) defines stiffness as follows:

385 If a numerical method [...] applied to a system
 386 with any initial conditions, is forced to use in
 387 a certain interval of integration a steplength
 388 which is excessively small in relation to the
 389 smoothness of the exact solution in that inter-
 390 val, then the system is said to be stiff in that
 391 interval.

392 A typical case of stiffness is for example, when
 393 different parts of the solution of a system of
 394 equations decays on different time scales.

395 This usually comes from very different scales
 396 inherent to the ODE. These scales will reflect in
 397 the parameters of the equations, i.e. the range of
 398 constants occurring in the equations of the systems.
 399 Therefore the stiffness of a system always depends
 400 not only on the mathematical form of the equa-
 401 tions but heavily on the magnitude of the constants
 402 occurring in them.

403 In principle it is possible to solve stiff equations
 404 with explicit methods, but this comes at the expense
 405 of a very small step size when using an adaptive
 406 step size algorithm and trying to achieve a certain
 407 accuracy. This in turn leads to high computational
 408 costs. For non-adaptive step size algorithms it leads
 409 to plain wrong results without the user knowing,
 410 since the algorithm still terminates, but with large
 411 error. Moreover, as the limited machine precision on
 412 a digital computer constitutes a lower bound for the
 413 step size, explicit methods usually become unstable
 414 when applied to stiff problems.

415 *Implicit methods*, on the other hand, do not use
 416 previous values to calculate the solution at the
 417 next grid point, but only employ them implicitly

in the form of the solution of a system of equa- 418
 tions. This makes implicit methods computationally 419
 much more costly, but usually allows a larger step 420
 size to be chosen, thus avoiding stability problems 421
 (Strehmel and Weiner, 1995). 422

In order to detect whether an explicit or implicit 423
 method is better suited for a given ODE we devise 424
 the following testing strategy. 425

First, we choose representative spike trains (drawn 426
 from a Poisson distribution) and compute approxi- 427
 mate solutions for the given system of ODEs using 428
 an explicit and implicit method of the same order: 429

1. an explicit 4th order Runge-Kutta method 430
2. an implicit Bulirsch-Stoer method of Bader and 431
 Deuffhard (Strehmel and Weiner, 1995) 432

both with adaptive step size. We can then compare 433
 them with respect to the required *average step size* 434
 and *minimal step size*. In cases where the implicit 435
 method performs better than the explicit method, 436
 we have reason to believe that the ODE is stiff and 437
 that the use of an implicit method is advisable. 438

Although ODEs may be stiff only for very spe- 439
 cific initial conditions, usually stiffness should be 440
 observable for a wide range of initial values, or 441
 in this case for a number of incoming spike trains 442
 (Strehmel and Weiner, 1995). By choosing many 443
 spike trains, evaluating the required step sizes for 444
 the implicit and explicit method for each of them, 445
 and comparing that to the machine precision ε , it is 446
 thus possible to detect whether the problem at hand 447
 is stiff or not. We propose the following rules for 448
 choosing an implicit algorithm: 449

- if the minimal step size of runs using the ex- 450
 plicit method is close to machine precision (i.e. 451
 less than $10 \cdot \varepsilon$) and this is not the case for the 452
 minimal step size of runs using the implicit 453
 method (i.e. greater than or equal to $10 \cdot \varepsilon$) this 454
 is a hint that the system of ODEs is possibly 455
 stiff. In this case an explicit stepping function 456
 could become unstable or even abort, so we 457
 suggest the use of an implicit algorithm. 458

- 459 • if the minimal step size of runs using the explicit
 460 method is reasonably large (i.e. greater
 461 than or equal to $10 \cdot \epsilon$) we have to test two
 462 cases:
- 463 • if the minimal step size of runs of the implicit
 464 method is very small (i.e. less than $10 \cdot \epsilon$),
 465 we suggest using an explicit method.
 - 466 • if the minimal step size of runs of the implicit
 467 method is large (i.e. greater than or equal to
 468 $10 \cdot \epsilon$), we go on to check if the average step
 469 size of runs using the implicit algorithm is
 470 much larger than the average step size of
 471 runs using the explicit algorithm. If this is
 472 the case, this again indicates that the system
 473 of ODEs is stiff and therefore choosing an
 474 implicit evolution method is advisable.

475 For a non-stiff system of ODEs, the computation
 476 time of an explicit algorithm should be lower, as it
 477 does not require the solution of a system of equations
 478 (Dahmen and Reusken, 2005). Therefore the
 479 choice of an explicit evolution method is sensible
 480 in cases where none of the above conditions are
 481 met. The algorithm that follows from these rules is
 482 depicted in Figure 2.

3 REFERENCE IMPLEMENTATION

483 In order to automate the process of finding the most
 484 appropriate solver for a given system of ODEs on
 485 a computer, we have designed and implemented
 486 an analysis toolbox in Python (<http://github.com/nest/ode-toolbox>). It builds on the formal
 487 mathematical foundations introduced in the
 488 previous sections and uses SymPy (Meurer et al.,
 489 2017) to carry out symbolic mathematical tests and
 490 transformations. To achieve a high degree of portability
 491 and re-usability, the input to the algorithm is
 492 given either in the form of JSON files or Python
 493 dictionaries, which specify equations, parameters
 494 and additional properties (for an example, see Section
 495 3.4). These two means of input allow an easy
 496 embedding of the toolkit into third-party tool chains
 497 and enable us to leverage the Python and SymPy
 498 parsers, which delegates all syntax checking and
 499

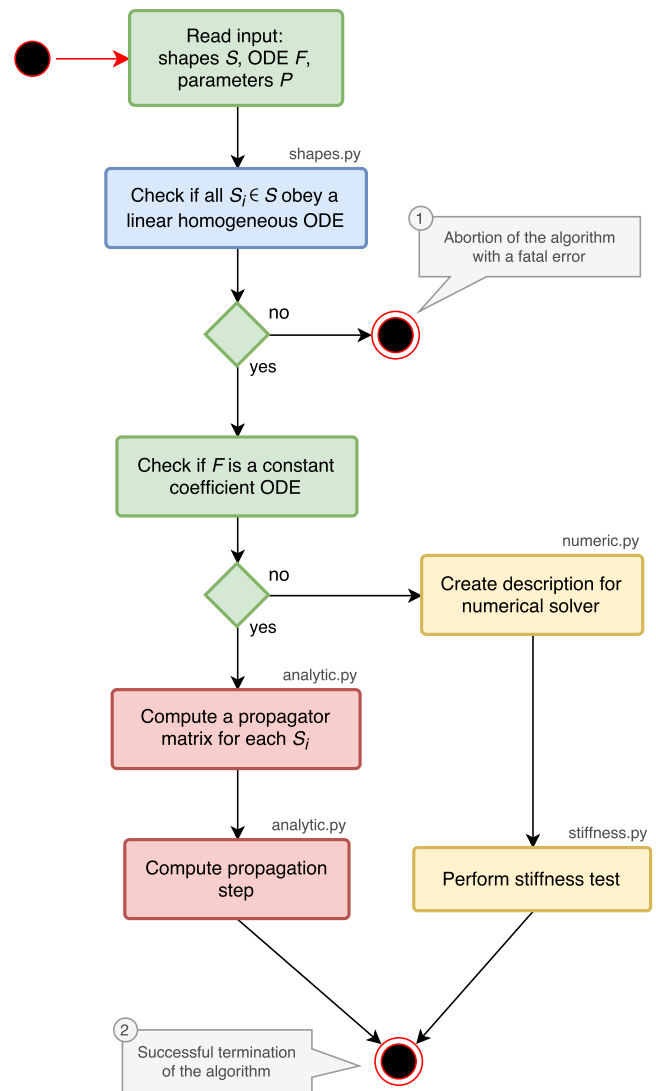


Figure 1. Activity diagram summarizing all steps of the ODE analysis algorithm. Steps executed in the main script of the toolbox are shown in green. The analysis of postsynaptic shapes (blue box) is detailed in Section 3.1. Parts shown in red represent the generation of an analytical solver, which is described in Section 3.2. The selection of a numerical stepper function is carried out by the yellow actions and explained in Section 3.3.

exception handling to well established and tested 500
 tools. 501

The algorithm expects three components in the 502
 input: i) an ODE describing the time evolution of 503
 a state variable (e.g. V), ii) a list of postsynaptic 504
 shapes (e.g. I) used within this ODE and specified 505
 either as functions of time or as ODEs with initial 506
 conditions and iii) a set of parameters with default 507

508 values for the equations. Fundamentally, the anal-
 509 ysis algorithm checks the given system of ODEs
 510 for membership of the following two major cate-
 511 gories and generates or selects an appropriate solver
 512 accordingly:

- 513 1. First order linear constant coefficient ODEs for
 514 the dynamics of a state variable (see Equation 4)
 515 whose inhomogeneous part is a postsynaptic
 516 shape (i.e. satisfies Equation 5) can be solved
 517 exactly using an analytical stepping scheme
 518 (Section 2.1).
- 519 2. All other systems of ODEs have to be solved
 520 by a numerical solver. ODEs in this category
 521 are, for example, non-linear ODEs describing
 522 the time evolution of a state variables, or lin-
 523 ear ODEs with an inhomogeneous part which
 524 is not a postsynaptic shape, i.e. not satisfying
 525 Equation 5.

526 The implementation of the analysis toolbox con-
 527 sists of different Python components which are
 528 introduced in the activity diagram in Figure 1. The
 529 main script orchestrates the execution of the analy-
 530 sis and uses the functions and classes of the different
 531 submodules:

532
 533 `shapes.py` contains classes and functions for analyz-
 534 ing and storing postsynaptic shapes either given
 535 as functions of time or ODEs with initial values
 536 (blue parts in Figure 1). The main algorithm in
 537 this module is explained in section Section 3.1.
 538 `analytic.py` provides the functionality to generate
 539 propagator matrices and compute a specifica-
 540 tion for the update step (red parts in Figure 1). A
 541 detailed description can be found in Section 3.2.
 542 `numeric.py` contains the code for creating a descrip-
 543 tion of the update step for further processing
 544 by the stiffness tester or a numerical stepper
 545 function (upper yellow box in Figure 1).
 546 `stiffness.py` implements the stiffness tester (lower
 547 yellow box in Figure 1). This module can ei-
 548 ther be used as a module within the analysis
 549 toolbox or a third-party tool, or run in a stand-
 550 alone fashion. It is explained in Section 3.3

together with the preparatory steps carried out 551
 in `numeric.py`. 552

The main script starts by reading and validating 553
 the input from a JSON file or a Python dictionary. 554
 It expects the keys `shapes`, `odes` and `parameters` to be 555
 present in the input. For each postsynaptic shape in 556
 the `shapes` section, it runs the algorithm described 557
 in Section 3.1, which checks if the given postsy- 558
 naptic shape obeys a linear homogeneous ODE and 559
 transforms it into a canonical representation suitable 560
 for further processing. If one of the postsynaptic 561
 shapes fails the test for linearity and homogeneity, 562
 the script terminates with an error (① in Figure 1), 563
 because this class of ODEs cannot be solved easily 564
 with traditional methods as explained in Section 6. 565

After processing the postsynaptic shapes, the 566
 script checks whether all equations in the `odes` sec- 567
 tion of the input are linear constant coefficient 568
 ODEs: the ODE is linear if the right hand side of 569
 the ODE differentiated twice by its symbol is zero, 570
 the coefficient of the symbol is constant if the right 571
 hand side of the ODE differentiated by its symbol 572
 is constant. If these two tests succeed, the system 573
 can be solved analytically (see Section 3.2). If one 574
 of them fails, a numerical stepper has to be chosen 575
 (Section 3.3). The output of the main script is again 576
 a Python dictionary or a JSON file, which contains 577
 a specification of the most appropriate solver for 578
 the given input (② in Figure 1). The remainder of 579
 this section explains the different algorithms in the 580
 submodules of the analysis toolbox. 581

3.1 Analysis of postsynaptic shapes 582

In the neuroscience literature, postsynaptic shapes 583
 are described either as functions of time or as ODEs 584
 with initial values. To provide users with maximum 585
 flexibility, both specifications are supported by our 586
 toolbox. Regardless of the form of the specification, 587
 each of the given postsynaptic shapes has to satisfy 588
 a linear, homogeneous ODE (Equation 5) to be 589
 solved either analytically or numerically. 590

In case the postsynaptic shape is given as an ODE 591
 with initial values, the check for linearity an ho- 592
 mogeneity is straightforward. For each occurring 593

594 derivative of the postsynaptic shape in the shape's
 595 definition, we simply have to iteratively subtract the
 596 product of the derivative and its factor from the orig-
 597 inal definition of the postsynaptic shape and check
 598 if the final difference is zero. This check fails if the
 599 postsynaptic shape is non-linear (i.e. at least one
 600 of the derivatives occurs as a power term) or not
 601 homogeneous (i.e. not all terms of the postsynaptic
 602 shape definition are products containing a deriva-
 603 tive of the shape). This check is implemented in the
 604 function `shape_from_ode()` in the `shape` module of the
 605 toolbox.

606 In case the postsynaptic shape is given as a func-
 607 tion of time, we check whether the function obeys
 608 a linear homogeneous ODE by trying to construct
 609 such an equation together with the initial values
 610 of all relevant derivatives. This procedure is imple-
 611 mented in the function `shape_from_function()` of the
 612 `shape` module. We start the evaluation by checking
 613 if the postsynaptic shape function obeys a linear
 614 homogeneous ODE of order 1.

```

1  t_value = None
2  ds = [shape, diff(shape, t)]
3  for t_ in range(1, max_t):
4      if ds[0].subs(t, t_) != 0:
5          t_value = t_
6          break
7
8  found_ode = False
9  if t_value is not None:
10     a0 = (1/ds[0] * ds[1]).subs(t, t_value)
11     diff_lhs_rhs = ds[1] - a0 * ds[0]
12     found_ode = diff_rhs_lhs == 0

```

615 In line 10 we calculate the factor a_0 from Equa-
 616 tion 6 by dividing the first derivative of the postsy-
 617 naptic shape by the shape at an arbitrary point t . To
 618 avoid a division by zero, we have to find a t so that
 619 the postsynaptic shape function is not zero at this
 620 t (lines 3-6). Line 11 calculates the difference be-
 621 tween the left and the right hand side of Equation 6.
 622 If this difference is zero (line 12) we know that the
 623 postsynaptic shape satisfies a linear homogeneous
 624 ODE of order 1. We also know the ODE itself by
 625 calculating its initial value in line 40 below.

626 If the postsynaptic shape does not obey a linear
 627 homogeneous ODE of order 1, we check if the

postsynaptic shape function satisfies a linear ho-628
 mogeneous ODE of a higher order. This test is run 629
 in a loop (line 15) that increments the order to check 630
 for each time Equation 5 is not satisfied. The loop 631
 terminates if either an ODE is found or `max_order` 632
 iterations are exceeded. The latter check prevents 633
 expensive tests of unlikely high orders. 634

```

13  order = 1
14  factors = [a0]
15  while not found_ode and order < max_order:
16      order += 1
17      ds.append(diff(ds[-1], t))
18      X = zeros(order)
19      Y = zeros(order, 1)

```

We start the loop by setting the next potential `order` 635
 (line 16), appending the next higher derivative of 636
 postsynaptic shape to the list of derivatives (line 17) 637
 and initializing the matrix \mathbf{X} with size `order` \times `order` 638
 (Equation 9, line 18) and the vector \mathbf{Y} with length 639
`order` (right hand side of Equation 10, line 19). 640

```

20  invertible = False
21  for t_ in range(max_t):
22      for i in range(order):
23          substitute = i + t_ + 1
24          Y[i] = ds[order].subs(t, substitute)
25          for j in range(order):
26              X[i, j] = ds[j].subs(t, substitute)
27
28      if det(X) != 0:
29          invertible = True
30      break

```

\mathbf{X} and \mathbf{Y} are assigned values according to Equa-641
 tions 9 and 10 (line 24 and 26) for varying $t =$ 642
 (t_1, \dots, t_n) (line 21) in order to find a t such that 643
 the matrix \mathbf{X} is invertible, i.e. $\det(\mathbf{X}) \neq 0$ (line 28). 644
 In the inner loop (line 22-26), t_i is substituted so that 645
 we first try $t = (1, \dots, n)$, second $t = (2, \dots, n+1)$ 646
 and so on (line 23). 647

If we find an invertible \mathbf{X} , we calculate the po-648
 tential factors a_i from Equation 5 according to 649
 Equation 11 for the current order we are checking 650
 for (`factors`, line 32). 651

```

31  if invertible:
32      factors = X.inv() * Y
33      diff_rhs_lhs = 0
34      for k in range(order):
35          diff_rhs_lhs -= factors[k] * ds[k]
36      diff_rhs_lhs += ds[order]
37      if diff_rhs_lhs == 0:

```

```

38     found_ode = True
39     break

```

Lines 33-36 calculate the difference between the left and the right hand side of Equation 5. If this difference is zero (line 37) we know that the postsynaptic shape satisfies an linear homogeneous ODE of order `order`.

If we do not find an ODE during the execution of the `while` loop, we terminate the algorithm with an error (① in Figure 1). If we do, we can go on to calculate the initial values of the postsynaptic shape equation by substituting t by 0 for all derivatives of the postsynaptic shape, which fully defines the found ODE.

```

40     iv = [x.subs(t, 0) for x in ds[:-1]]

```

In the case of successful termination, the functions `shape_from_ode()` and `shape_from_function()` both return a `Shape` object to the main script of the toolbox, which encapsulates all attributes of the postsynaptic shape required for further processing.

3.2 Generation of an analytical evolution scheme

If the ODE describing the update of a state variable was found to be a constant coefficient ODE and all postsynaptic shapes obey linear homogeneous ODEs, we can solve the system of ODEs analytically according to Section 2.1. To this end, the module `analytic` provides a class `Propagator`, which has two member functions corresponding to the two steps required for the generation of an analytical evolution scheme.

The function `compute_propagator_matrices()` takes an ODE and a list of `Shape` objects and computes a propagator matrix (Equation 17) for each postsynaptic shape. These matrices can be used to evolve the system from one point to the next. The basic idea here is to populate the matrix `A` using the factors of the derivatives (`factors`, computed in lines 12 and 31 of the code in Section 3.1), the factor of the postsynaptic shape used in the ODE for the state variable (`ode_shape_factor`) and the factor of the symbol of the ODE (`ode_sym_factor`). For the equation

$$\frac{d}{dt}V = \frac{1}{\tau} \cdot V + \frac{1}{C_1} \cdot I_1 + \frac{1}{C_2} \cdot I_2$$

`ode_sym_factor` would thus be $\frac{1}{\tau}$. It is calculated using the following line of code:

```

1     ode_sym_factor = diff(ode_def, ode_symbol)

```

`ode_shape_factor` would be $\frac{1}{C_1}$ for postsynaptic shape I_1 in the example equation and $\frac{1}{C_2}$ for I_2 . As these factors and other parameters depend on the postsynaptic shape, we run the following code in a loop (omitted for better readability), each iteration assigning the current `Shape` object to the variable `shape`:

```

2     ode_shape_factor = diff(ode_def, shape.symbol)
3
4     if shape.order == 1:
5         A = Matrix([
6             [shape.factors[0], 0],
7             [ode_shape_factor, ode_sym_factor]])
8     elif shape.order == 2:
9         pq = -shape.factors[1] / 2 +
10            ↪ sqrt(shape.factors[1]**2 / 4 +
11            ↪ shape._factors[0])
12         A = Matrix([
13             [shape.factors[1] + pq, 0, 0],
14             [1, -pq, 0],
15             [0, shape_factor, ode_sym_factor]])
16     else:
17         order = shape.order
18         A = zeros(order + 1)
19         A[order, order] = ode_sym_factor
20         A[order, order - 1] = shape_factor
21         for j in range(0, order):
22             A[0, j] = shape.factors[order - j - 1]
23         for i in range(1, order):
24             A[i, i - 1] = 1

```

Line 2 computes the `ode_shape_factor` for the current postsynaptic shape. In order to make the calculation of the solution more efficient (i.e. using fewer arithmetic operations on a computer), `compute_propagator_matrices()` creates a lower triangular matrix for postsynaptic shapes of order 1 and 2 (lines 5-7 and 9-13, respectively) as explained in Equation 14 and a generic matrix for all higher orders according to Equation 13 (lines 15-22). The variable `pq` in line 9 corresponds to Equation 15.

710 The propagator matrix for each postsynaptic shape
 711 can now be computed by taking the matrix exponen-
 712 tial of the matrix \mathbf{A} multiplied by the update step
 713 size h :

```
23 propagator_matrices.append(exp(A * h))
```

714 The second function of the `Propagator` class,
 715 `compute_propagation_step()`, takes the list of propaga-
 716 tor matrices and postsynaptic shapes and computes
 717 a calculation specification that can be executed to
 718 actually perform the system update. As this function
 719 merely runs a loop over all propagator matrices and
 720 generates the update instructions as a list of strings,
 721 the code is omitted here.

722 3.3 Finding an appropriate numerical 723 solver

724 In case the differential equation describing the
 725 dynamics of a state variable was not found to be a
 726 linear constant coefficient ODE, the system must
 727 be evolved using a numerical stepping scheme as
 728 explained in Section 2. Instead of a full calculation
 729 specification, as produced for the analytical solution
 730 in Section 3.2, the `numeric` module of the toolbox
 731 just passes the specification of ODEs from the in-
 732 put and the `Shape` objects created by the algorithm
 733 in Section 3.1 on to the stiffness tester, which is
 734 implemented in the `stiffness` module.

735 The stiffness tester uses the standard Python mod-
 736 ules SymPy and NumPy for symbolic and numeric
 737 calculations. For evolving the ODEs during the
 738 test procedure, it currently uses PyGSL, a Python
 739 wrapper around the GNU Scientific Library (GSL;
 740 Gough, 2009). This library was chosen over more
 741 pythonic alternatives such as SciPy due to its more
 742 comprehensive selection of ODE solvers.

743 The stiffness tester executes the algorithm de-
 744 scribed in Section 2.2 and gives a recommendation
 745 as to whether the use of an explicit or an implicit
 746 evolution scheme is appropriate. The steps per-
 747 formed by the algorithm are shown in Figure 2.
 748 The choice of the factor 6 for comparing average
 749 step sizes of the explicit and the implicit schemes is
 750 motivated in Section 3.3.1. For the evolution of the

system of ODEs, the equations receive representa- 751
 tive spike trains drawn from a Poisson distribution 752
 with a rate of $\nu = 0.1 \text{ s}^{-1}$ and inter-spike intervals 753
 distributed around $\frac{1}{\nu}$ (Connors and Gutnick, 1990). 754

3.3.1 Comparison of average step sizes 755

When comparing average step sizes of the im- 756
 plicit and explicit method applied to a certain set 757
 of ODEs, we assume that the set of ODEs is stiff 758
 when the average step size of the implicit method 759
 is considerably larger than the average step size 760
 of the explicit method, see Section 2.2, i.e. when 761
 $s_{\text{implicit}} > \beta \cdot s_{\text{explicit}}$ for some β . 762

To determine an appropriate factor β , we devel- 763
 oped a testing strategy using a well known example 764
 of a set of stiff ODEs: with $a = -100$ and initial 765
 values $y_1(0) = y_2(0) = 1$, 766

$$\begin{aligned} \frac{dy_1}{dt} &= ay_1 & (20) \\ \frac{dy_2}{dt} &= -2y_2 + y_1 \end{aligned}$$

is a typical stiff ODE system (example taken from 767
 Dahmen and Reusken, 2005). The solution $y_1(t) = 768$
 e^{-100t} decays very quickly, whereas the solution 769
 $y_2(t) = -\frac{1}{98}e^{-100t} + \frac{99}{98}e^{-2t}$ decreases a lot more 770
 slowly, which causes the stiffness of this system. 771

y_1 is already reduced by four decimal places at 772
 $t = 0.1$ and y_1 is practically negligible for even 773
 larger t . Nevertheless, it plays a major role in the 774
 calculation of y_2 when using an explicit integration 775
 method. Using a simple explicit Euler method and 776
 a resolution h for the approximation \tilde{y}_1 of y_1 , we 777
 have the following recursive specification: 778

$$\tilde{y}_1(t+h) = \tilde{y}_1(t) - 100h\tilde{y}_1(t) = (1 - 100h)\tilde{y}_1(t).$$

For $h = \frac{1}{200}$ and $t = \frac{1}{10}$ we get 779

$$\tilde{y}_1(1/10) = 2^{-20} < 10^{-6}.$$

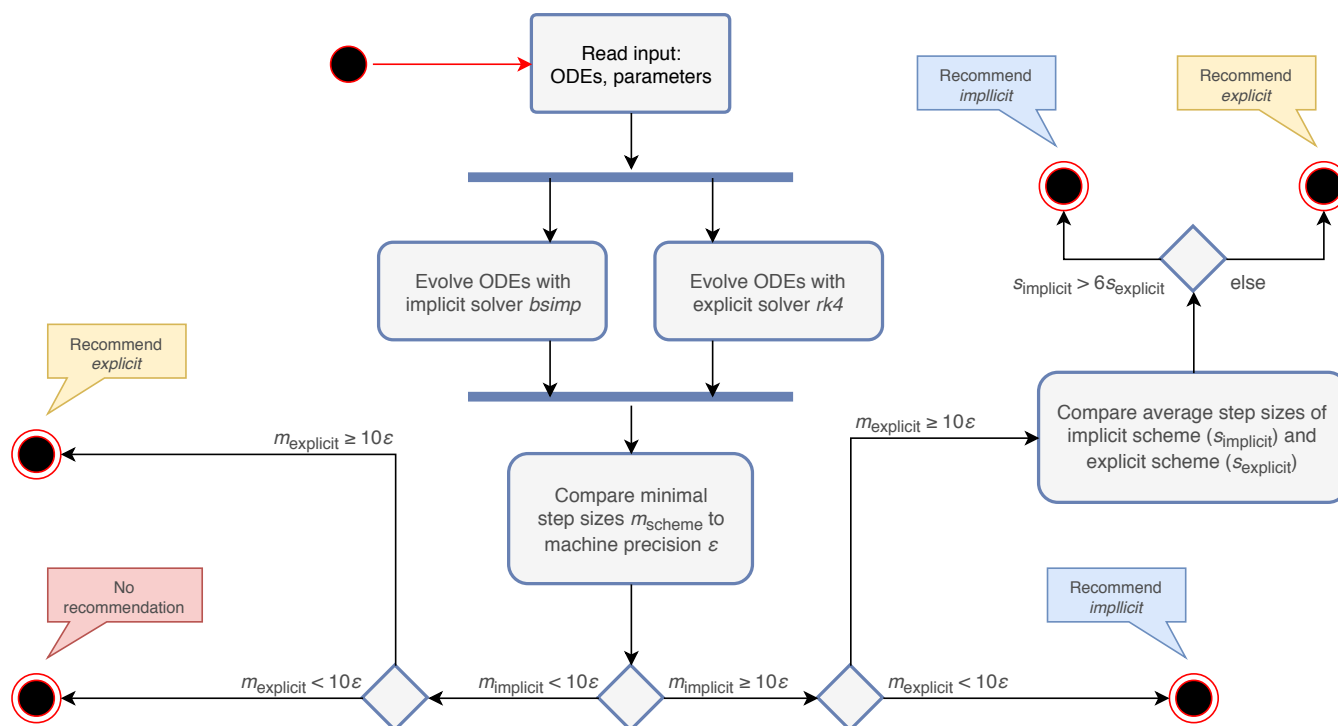


Figure 2. Activity diagram summarizing the steps taken to recommend an appropriate numerical stepping scheme. The input to the algorithm are the ODEs and their parameters. After evolving the system of ODEs in parallel with an implicit and an explicit solver, it compares the minimal step sizes (m_{scheme}) of each scheme with the machine precision (ϵ). Depending on the outcome of the comparison, it recommends an appropriate stepping scheme (explicit or implicit) or compares the average step sizes (s_{scheme}) of the tested schemes. In the case that both the step size of the explicit and implicit solver are close to ϵ , the algorithm does not give a recommendation, but terminates with a warning instead.

780 For computational efficiency, we would like to
 781 choose a larger step size for y_2 since the solution
 782 decays a lot slower than y_1 . If we therefore choose
 783 $h = \frac{1}{2}$ to integrate y_2 , we get

$$\tilde{y}_1(t+h) = -49\tilde{y}_1(t),$$

784 causing an explosive growth in the course of the
 785 calculations.

786 A stiff set of ODEs will always result in the av-
 787 erage step size of an implicit method exceeding by
 788 far the average step size of a comparable explicit
 789 method. Hence the runtime of the implicit method
 790 should be less than the explicit method's runtime.
 791 However, runtime is not solely affected by the grade
 792 of stiffness, so the stiffness of a given set of ODEs
 793 is evaluated more accurately by comparing average
 794 step sizes.

To isolate stiffness from other factors, we chose
 Equation 20 for its simplicity. This problem is
 clearly stiff, as described above, and the grade of
 stiffness relates directly to the size of the factor a .
 Therefore it can be used as a controlled stiff problem
 where other effects coming from the complexity of
 the system do not play a role.

We measure the runtimes of the implicit and the
 explicit methods (using the corresponding GSL-
 solvers) for five runs over 20 milliseconds each,
 whilst systematically varying the stiffness control-
 ling parameters a and the resolution h . The quotient
 of the average implicit and explicit runtimes is
 shown in Figure 3.

For each measurement series, we can determine
 a^* , the value of a for which the runtimes of the
 explicit and the implicit evolution scheme are the
 same. We then calculate the ratio of the step sizes
 employed by the implicit and explicit schemes at a^* :

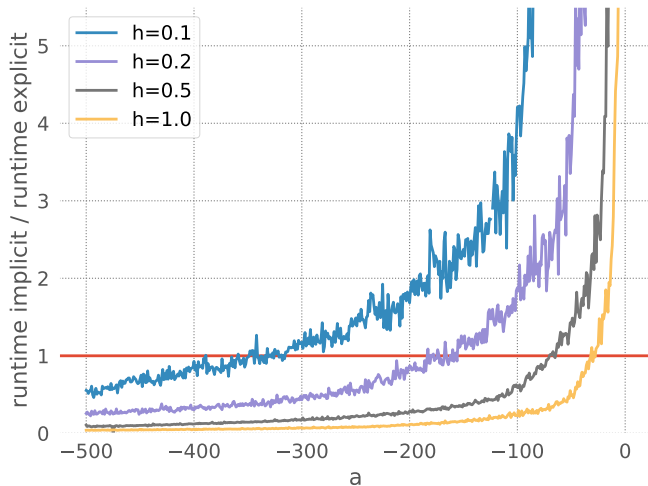


Figure 3. Comparison of implicit and explicit methods for a stiff ODE. Ratio of runtimes for the implicit and explicit method as a function of the factor a in Equation 20, for varying resolutions h and a desired accuracy of 10^{-3} . Curves averaged over 5 runs of 20 ms each. The red bar indicates when the explicit and implicit methods require the same amount of time to evolve the ODE system. Where a curve is below the red bar, the implicit method is faster than the corresponding explicit method.

814 $r^* = \frac{s_{\text{implicit}}(a^*)}{s_{\text{explicit}}(a^*)}$. Because in this problem the run-
 815 time, stiffness and step size are solely influenced by
 816 the factor a , we can consider r to be the borderline
 817 factor, i.e. problems with $s_{\text{implicit}} > r^* \cdot s_{\text{explicit}}$ are
 818 sufficiently stiff to make the implicit method faster.

819 For all the curves in Figure 3, we determine a
 820 value for r^* between 6 and 7. As some input sce-
 821 narios may result in a somewhat stiffer system than
 822 that brought about by the representative spike train
 823 chosen in the stiffness tester, we choose $\beta = 6$ con-
 824 servatively on the low side of the range of r^* , to
 825 ensure that the implicit scheme is used in all stiff
 826 cases.

827 3.4 Example

828 The use of the toolbox as a Python module
 829 is explained in detail in the `README.md` file of the
 830 git repository at [http://github.com/nest/](http://github.com/nest/ode-toolbox)
 831 `ode-toolbox`. Here, we demonstrate the use of
 832 the analysis toolbox by executing the script file
 833 `ode_analyzer.py` in a stand-alone fashion for generat-
 834 ing a solver specification for a conductance-based

integrate-and-fire neuron with alpha-shaped postsy-835
 naptic conductances. The script expects the name 836
 of a JSON file as its only command line argument: 837

```
python ode_analyzer.py iaf_cond_alpha.json
```

The file `iaf_cond_alpha.json` is shown in Listing 1.838
 It contains the specification of one differential equa-839
 tion for the membrane potential v_m in the `odes` 840
 section in lines 3-7. This section is a list and can 841
 potentially contain multiple ODEs. The `shapes` sec-842
 tion defines two postsynaptic shapes, one of which 843
 is specified as a function of time (`g_in`, lines 10-14), 844
 the other as an ODE with initial conditions (`g_ex`, 845
 lines 15-20). The parameters and their default val-846
 ues are given in the `parameters` dictionary in lines 847
 22-33. This dictionary maps default values to pa-848
 rameter names and has to contain an entry for each 849
 free variable occurring in the equations given in the 850
`odes` or `shapes` sections. 851

Depending on the complexity of the ODEs and 852
 postsynaptic shapes contained in the input, the anal-853
 ysis may take some time. During its execution, 854
 the analysis tool prints diagnostic messages about 855
 the current processing steps. If all steps succeed, 856
 it writes the result again to a JSON file, which 857
 can be read by the next tool in the model gen-858
 eration pipeline to create the a complete model 859
 implementation. 860

For the input shown in Listing 1, the analysis 861
 toolbox produces the following output: 862

```
1 {
2   "solver": "numeric-explicit"
3   "shape_ode_definitions": [
4     "-1/tau_syn_in**2 * g_in + -2/tau_syn_in *
5     ↪ g_in_d",
6     "-1/tau_syn_ex**2 * g_ex + -2/tau_syn_ex *
7     ↪ g_ex_d"
8   ],
9   "shape_state_variables": [
10    "g_in_d",
11    "g_in",
12    "g_ex_d",
13    "g_ex"
14  ],
15  "shape_initial_values": [
16    "0",
17    "e/tau_syn_in",
18    "0",
19    "e/tau_syn_ex"
```

```

1  {
2    "odes": [
3      {
4        "symbol": "V_m",
5        "definition": "(-(g_L*(V_m-E_L))-(g_ex*(V_m-E_ex))-(g_in*(V_m-E_in))+I_stim+I_e)/C_m",
6        "initial_values": ["E_L"]
7      }
8    ],
9    "shapes": [
10     {
11       "type": "function",
12       "symbol": "g_in",
13       "definition": "(e/tau_syn_in)*t*exp((-1)/tau_syn_in*t)"
14     },
15     {
16       "type": "ode",
17       "symbol": "g_ex",
18       "definition": "(-1)/(tau_syn_ex)**(2)*g_ex+(-2)/tau_syn_ex*g_ex'",
19       "initial_values": ["0", "e / tau_syn_ex"]
20     }
21   ],
22   "parameters": {
23     "V_th": -55.0,
24     "g_L": 16.6667,
25     "C_m": 250.0,
26     "E_ex": 0,
27     "E_in": -85.0,
28     "E_L": -70.0,
29     "tau_syn_ex": 0.2,
30     "tau_syn_in": 2.0,
31     "I_e": 0,
32     "I_stim": 0
33   }
34 }

```

Listing 1. Example JSON file as input to the analysis toolbox. The file contains three entries: `odes` describing the ODEs of the system, `shapes` containing the postsynaptic shapes used in the ODEs and `parameters` specifying the parameters and default values for the differential equations in the `shapes` and `odes` sections.

```

18  ],
19  }

```

863 The meaning of the fields is explained in detail in
864 the `README.md` of the toolbox.

4 RESULTS

865 To evaluate the proposed framework for the seman-
866 tic analysis of a system of ODEs and assessment of
867 its stiffness we have chosen two approaches. One
868 was to apply the stiffness tester to the neuron models
869 currently implemented in the NEST Modeling Lan-
870 guage (NESTML; Plotnikov et al., 2016), the other
871 was to compare runtimes of explicit and implicit
872 evolution schemes applied to two commonly used
873 simplified versions of the Hodgkin-Huxley model.

The stiffness tester was integrated and success-874
fully used in the tooling for NESTML, a domain 875
specific language for the definition of neuron mod-876
els for the neuronal simulator NEST (Gewaltig and 877
Diesmann, 2007; Kunkel et al., 2017). NESTML is 878
built using MontiCore (e.g. Krahn, 2010; Grönniger 879
et al., 2008). MontiCore is a language work-880
bench (Erdweg et al., 2013) that enables an agile 881
and incremental implementation of lightweight 882
DSLs including the symbol table functionality (Mir 883
Seyed Nazari, 2017), code generation facilities (e.g. 884
Schindler, 2012; Rumpe, 2017) and support for edi-885
tors in Eclipse IDE (e.g. Völkel, 2011; Krahn et al., 886
2007). NEST's focus is on the simulation of the 887
dynamics of large networks of spiking neurons (e.g. 888
Potjans and Diesmann, 2012; van Albada et al., 889
2015; Kunkel et al., 2010). Neuron models in NEST 890

891 are usually rather simple point neurons or models
 892 with a few electrical compartments instead of rich
 893 compartmental neurons built from morphologically
 894 detailed reconstructions. The simulator is capable of
 895 running on a large range of computer architectures
 896 ranging from laptops over standard workstations to
 897 the largest supercomputers available today (Kunkel
 898 et al., 2014).

899 Within NESTML, the analysis toolbox developed
 900 in Sections 2 and 3 is used for the numerical analy-
 901 sis of neuron models defined as systems of ODEs
 902 and provides either the implementation of an effi-
 903 cient and accurate analytical integration scheme or
 904 recommends a good numerical solver. Therefore it
 905 allows the simulation of a large variety of biological
 906 neuron models in NEST.

907 As a simple yet meaningful validation of the stabil-
 908 ity checks introduced in Section 2.2, we applied the
 909 stiffness tester to all neuron models currently imple-
 910 mented in NESTML (see <https://github.com/nest/nestml/tree/master/models>). The re-
 911 sult of this evaluation is that with default
 912 parametrization, the systems of ODEs of all neu-
 913 ron models are non-stiff and can thus be safely
 914 integrated using an explicit numerical integration
 915 scheme without any detrimental effects on effi-
 916 ciency and accuracy. This is a reassuring finding,
 917 as it indicates that previous studies using these neu-
 918 ron models are unlikely to contain distorted results
 919 due to numeric instabilities in the integration, for a
 920 counter-example see Pauli et al. (2018).
 921

922 However, when the default parametrization is
 923 slightly altered, the stiffness test finds that some
 924 systems of ODEs are now evaluated as being stiff,
 925 which suggests that the choice of an implicit evo-
 926 lution scheme would be more advisable than the
 927 default choice. Figure 4 summarizes these observa-
 928 tions for a selection of six commonly used neuron
 929 models and shows how a systematic change of one
 930 parameter in these models results in an evaluation
 931 as stiff or non-stiff.

932 As a second test, we apply the stiffness tester
 933 to the Fitzhugh-Nagumo and Morris-Lecar models
 934 (FitzHugh, 1961; Nagumo et al., 1962; Morris and

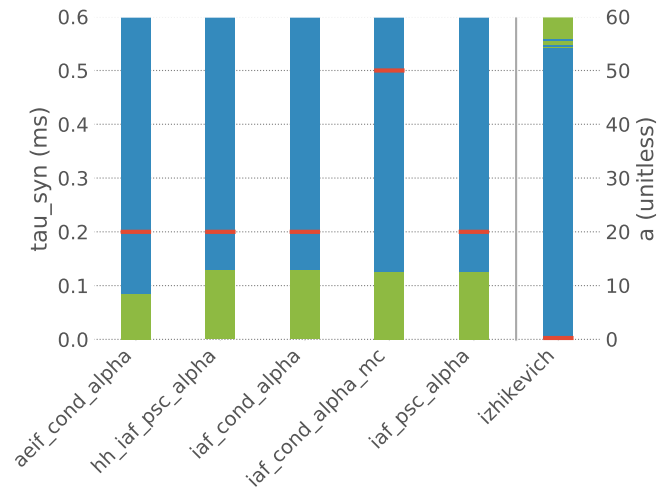


Figure 4. Results of the stiffness test for six neuron models from NEST. Red bars indicate the default value of the selected parameter in NEST, blue indicates the value range in which the system of ODEs evaluates as non-stiff, green indicates the range in which it evaluates as stiff. `aeif_cond_alpha` is a conductance-based adaptive exponential integrate-and-fire model with alpha-shaped postsynaptic conductances, `hh_iaf_psc_alpha` a Hodgkin-Huxley type model with alpha-shaped postsynaptic currents, `iaf_cond_alpha` a conductance-based integrate-and-fire neuron with alpha-shaped postsynaptic conductances, `iaf_cond_alpha_mc` a conductance-based integrate-and-fire neuron with alpha-shaped postsynaptic conductances and multiple compartments, `iaf_psc_alpha` a current-based integrate-and-fire neuron with alpha-shaped postsynaptic currents and `izhikevich` the model dynamics proposed by Izhikevich (2003). The test was applied to the ODE systems for varying values of the parameter τ_{syn} of the first five models and for the parameter a of the last model.

Lecar, 1981), non-linear oscillators that include the generation of an action potential as part of the dynamics, rather than applying an artificial threshold as many point neuron models do. To assess the comparative performance of the two approaches, we vary both the stiffness controlling parameter of the model equations and the resolution h , as a parameter of the stiffness tester (`stiffness.py`; see Section 3). For small values of h , the explicit approach is expected to exhibit a better performance as it is relatively easy to find the solution, and the explicit approach is computationally less expensive. As h increases, it becomes harder to determine the

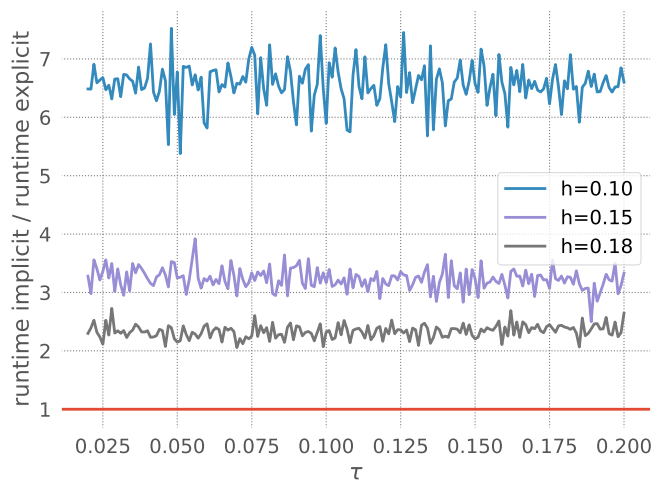


Figure 5. Application of the stiffness tester to the Fitzhugh-Nagumo model. Ratio of runtimes for the implicit and explicit method as a function of the factor τ in Equation 21, for varying resolution h and a desired accuracy of 10^{-5} . Curves averaged over 5 runs of 20 ms each. Red bar as in Figure 3.

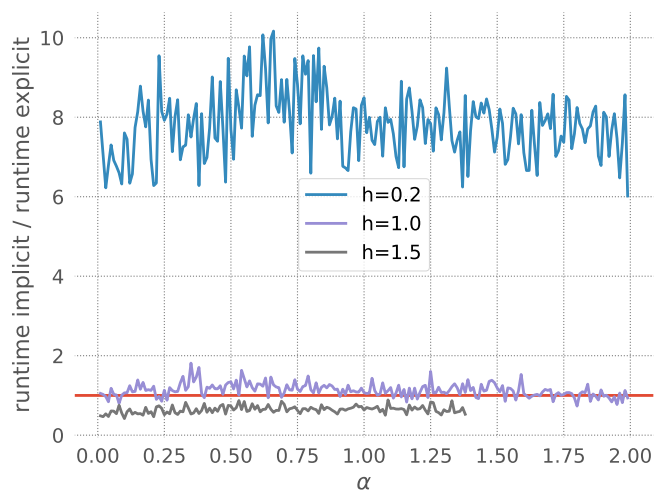


Figure 6. Application of the stiffness tester to the Morris-Lecar model. Ratio of runtimes for the implicit and explicit method as a function of the factor ε in Equation 22, for varying resolution h and a desired accuracy of 10^{-5} . Curves averaged over 5 runs of 20 ms each. Red bar as in Figure 3.

948 correct solution, so that the more expensive, but
 949 more reliable, implicit method becomes advanta-
 950 geous. Alternatively, a systematic variation of the
 951 desired accuracy would yield the same insight (data
 952 not shown).

Figure 5 demonstrates a comparison of the im-953
 plicit and explicit methods applied to the FitzHugh-954
 Nagumo model. The model comprises two vari-955
 ables, one for the membrane potential V and a 956
 recovery variable W . The dynamics are given by: 957

$$\begin{aligned} V' &= V - \frac{1}{3}V^3 - W + 0.25 \\ W' &= \tau(V + 0.7 - 0.8W). \end{aligned} \quad (21)$$

The figure shows the quotient of the time that 958
 the corresponding GSL-solvers for the explicit and 959
 implicit methods spent on integrating the ODE sys-960
 tem for 20 milliseconds with a desired accuracy of 961
 10^{-5} . For all resolutions shown in Figure 5, the 962
 explicit scheme is faster, and is also the approach 963
 recommended by our toolbox. As the resolution be-964
 comes coarser (increased values of h), the curves 965
 shift down towards the point at which the implicit 966
 method would be faster. For $h > 0.185$, our toolbox 967
 recommends an implicit approach, and indeed in 968
 such cases the explicit scheme, as implemented by 969
 the GSL, exits with an error. This is due to the vari-970
 able V becoming so large in one of the internal steps 971
 that it can no longer be represented by a double.972
 For a higher required accuracy of 10^{-10} , all curves 973
 shift to below the red line (data not shown), and 974
 the toolbox recommends an implicit solver for all 975
 tested resolutions. 976

We apply the same approach to the Morris-Lecar 977
 model (Morris and Lecar, 1981): 978

$$\begin{aligned}
 V' &= I + 2W(-0.7 - V) + 0.5(-0.5 - V) \\
 &\quad + 1.1m(V)(1 - V) \\
 W' &= \alpha\lambda(V)(w(V) - W) \\
 m(V) &= \frac{1}{2} \left(1 + \tanh \left(\frac{V + 0.01}{0.15} \right) \right) \\
 w(V) &= \frac{1}{2} \left(1 + \tanh \left(\frac{V + 0.12}{0.3} \right) \right) \\
 \lambda(V) &= \cosh \left(\frac{V - 0.22}{2 \cdot 0.3} \right),
 \end{aligned} \tag{22}$$

979 where I represents injected current. Figure 6
 980 shows that for a resolution of $h = 0.2$, the explicit
 981 solver is faster, but for larger values of h the im-
 982 plicit solver becomes more efficient. Accordingly,
 983 our toolbox recommends explicit for the former and
 984 implicit for the latter. Note also that the explicit
 985 solver **exits with an overflow error** for $h = 1.5$ with
 986 values of α above 1.4. Again, the toolbox catches
 987 this risk of numerical instability and recommends
 988 the implicit scheme.

989 These results show that the toolbox can correctly
 990 assess where it is safe and efficient to use an ex-
 991 plicit scheme, and where an implicit scheme would
 992 be appropriate, either for reasons of speed or for
 993 numerical stability.

5 RELATED WORK

994 In this section we compare our proposed frame-
 995 work for choosing evolution schemes for systems
 996 of ODEs in neural models with the correspond-
 997 ing approaches implemented in the simulators
 998 Brian (Goodman and Brette, 2009; Stimberg et al.,
 999 2014) and NEURON (Hines and Carnevale, 2000;
 1000 Carnevale and Hines, 2006). These two simula-
 1001 tors were chosen as they are in wide-spread use
 1002 in the community. We will further consider the ap-
 1003 plication of software for symbolic computation (for

exact mathematical calculations) or scientific com-1004
 puting (for numerical calculations) to our setting in1005
 language modelling for neural simulators. 1006

5.1 Brian

1007

Similar to our framework, the implementa1008
 of the Brian simulator also makes a distinction1009
 between systems of ODEs that can be solved an1010
 alytically and systems that can only be solved1011
 efficiently in a numeric manner. In addition to1012
 simple integrate-and-fire neurons, Brian also sup1013
 ports multi-compartmental neurons and neurons1014
 described by stochastic ODEs. As these types of1015
 models cannot be currently analyzed by our ODE1016
 analysis toolbox, we will not take them into account1017
 here. Instead we focus on single-compartmental de1018
 terministic neuron models as we can only draw a1019
 meaningful comparison for this group of neuron1020
 models. 1021

In Brian, neuron dynamics can be described by1022
 a system consisting of ODEs and time-dependent1023
 functions. They are either classified as *linear*, mean1024
 ing they can be solved analytically, or as *non-linear*1025
 meaning they cannot be solved analytically and1026
 must be solved numerically using the *forward Eu*1027
ler method (if not stated otherwise by the author1028
 of the model). In theory, linear constant coefficient1029
 ODEs can be solved analytically by Brian. However1030
 if the dynamics of a neuron are described using a1031
 non-constant function of time rather than an ODE1032
 defining this function they are always solved nu1033
 merically. This could be improved by using our1034
 proposed framework, which allows an analytical1035
 solver to be generated even for a system consist1036
 ing of time-dependent functions that satisfy a linear1037
 homogeneous ODE and feed into a linear constant1038
 coefficient ODE. Our framework thus allows an1039
 analytical evolution for a larger class of neuron1040
 dynamics. In particular, our framework seems to1041
 be more robust with respect to the use of several1042
 different postsynaptic shapes, as they are treated1043
 separately in contrast to Brian's approach, where1044
 the system is analyzed by SymPy as a whole. 1045

1046 All systems of ODEs in Brian that are not evolved
 1047 by an analytical evolution scheme are by default
 1048 evolved using the simple Euler method. To cir-
 1049 cumvent this, it is possible to choose a numerical
 1050 evolution scheme from a list of other methods. This
 1051 approach works well for users who are aware of the
 1052 numerical consequences of their choice of solver but
 1053 can be problematic for scientists who lack the abil-
 1054 ity to weigh up the advantages and disadvantages
 1055 of different numerical evolution schemes for their
 1056 particular system of ODEs. Moreover, as demon-
 1057 strated in Figure 3, the choice of an appropriate
 1058 evolution scheme might depend on the exact param-
 1059 eters for the ODEs and thus not be obvious even for
 1060 an advanced user.

1061 5.2 NMODL

1062 NMODL is the model specification language of
 1063 the NEURON simulator. NEURON was created
 1064 for describing large multi-compartmental neuron
 1065 models and thus also supports a wider range of
 1066 models than our proposed framework currently does.
 1067 We will again only contrast those types of models
 1068 for which a comparison is meaningful.

1069 For linear systems of ODEs, NMODL chooses
 1070 an evolution method that propagates the system
 1071 by evolving each variable under the assumption
 1072 that all other variables are constant during one time
 1073 step. In many cases this approach approximates
 1074 the true solution well, but it is still less accurate
 1075 than an actual analytical solution. For all other sys-
 1076 tems of ODEs, i.e. all non-linear ODEs, an implicit
 1077 method is chosen, regardless of the exact proper-
 1078 ties of the equations to guarantee an evolution of
 1079 stiff ODEs without causing numeric instabilities.
 1080 This is a robust solution but may lead to excessively
 1081 large simulation run times in cases where the choice
 1082 of an explicit evolution scheme for non-stiff ODE
 1083 systems would be sufficient.

1084 5.3 Software for symbolic computation 1085 and scientific computing

1086 There are a number of high quality and widely
 1087 used applications available for symbolic computa-
 1088 tion, most notably *Wolfram Mathematica* (Benker,

2016), *Modelica* (Tiller, 2001) and *Maple* (West-
 1089 ermann, 2010). All three provide frameworks for
 1090 solving ordinary differential equations both sym-
 1091 bolically and numerically. Here, we will briefly
 1092 describe their capabilities and limitations for both
 1093 symbolic and numeric integration of systems of
 1094 ODEs. 1095

5.3.1 Symbolic integrators 1096

At first appearance the integration schemes pro-
 1097 vided by the programming languages (or in the case
 1098 of Modelica, modelling language) seem appropriate
 1099 for the task addressed in our study. As discussed in
 1100 Section 1, the ordinary differential equations used
 1101 to define neuron models and to describe their dy-
 1102 namical behaviour are typically linear (though not
 1103 homogeneous and not linear with a constant coeffi-
 1104 cient) and can in several cases be solved analytically
 1105 by any of the programs above. However, for the
 1106 specific requirements related to neural simulations,
 1107 there are several reasons why they are not entirely
 1108 well suited. 1109

Firstly, neurons receive input that generally
 1110 changes in every integration step due to the arrival
 1111 of incoming spikes, thus changing the differential
 1112 equations to be solved. Although each of these dif-
 1113 ferential equations can be integrated easily using
 1114 e.g. Wolfram Mathematica, none of these frame-
 1115 works provide a general, exact solution for each
 1116 integration step, that takes a run-time generated
 1117 varying input into account. The next two points
 1118 are related to the size of neural systems commonly
 1119 investigated. Spiking neuronal network models of
 1120 ten contain of the order of $10^3 - 10^5$ neurons, and
 1121 sometimes substantially more (Kunkel et al., 2014).
 1122 Calling external software for symbolic computa-
 1123 tion of ordinary differential equations during run-
 1124 time for each neuron is therefore often too costly.
 1125 Moreover, for large models, the simulation soft-
 1126 ware is likely to be deployed on a large cluster or
 1127 supercomputer. The aforementioned applications
 1128 are typically not installed on such architectures,
 1129 whereas Python is a standard installation, providing
 1130 the package SymPy, which is sufficient for symbolic
 1131 computation in this context. 1132

1133 5.3.2 Numerical integrators

1134 There are a number of approaches to automatically
 1135 select numeric integrators depending on whether
 1136 the problem is stiff or non-stiff (Shampine, 1983,
 1137 1991; Petzold, 1983). These approaches are typi-
 1138 cally designed to switch integration schemes during
 1139 runtime when the problem changes its properties.
 1140 All of them rely in one way or another on the be-
 1141 haviour of the Jacobian matrix evaluated at the point
 1142 of integration. Typically, the methods try to approxi-
 1143 mate the dominant eigenvalue of the Jacobian with a
 1144 low cost compared to that of the stepping algorithm.
 1145 However, for a spiking neural network simulation,
 1146 the determination of the stiffness of the system, and
 1147 thus the solver, should occur before the simulation
 1148 starts, as to minimize runtime costs.

1149 Thus the question remains whether it would be
 1150 possible to carry out these kind of tests during gen-
 1151 eration of the neuron model. Applying the test to
 1152 a large number of randomly selected values of the
 1153 state variables, or carrying out a number of test runs
 1154 using representative spike trains would allow to
 1155 work around the fact that the solution up to a given
 1156 point is not yet known. However, as these tests rely
 1157 on determining the stiffness through the properties
 1158 of the Jacobian, they would still not be completely
 1159 precise. As we have the advantage of effectively
 1160 no computational constraints during generation of
 1161 the neuron model, there is thus no advantage by
 1162 using such a low-cost strategy. In our approach
 1163 we compute the solution using both explicit and
 1164 implicit schemes and compare their behavior a pos-
 1165 teriori, thus obtaining an accurate assessment of the
 1166 appropriate solver for a given set of parameters.

1167 In addition, as for symbolic integration, the pack-
 1168 ages that provide such stiffness testing capability for
 1169 numeric integration do not provide a framework for
 1170 handling a run-time determined variable input due
 1171 to incoming spikes. Thus we conclude that the spe-
 1172 cific problem addressed by our toolbox lies outside
 1173 the scope of general purpose symbolic and numeric
 1174 integration packages.

6 DISCUSSION

We have presented a novel simulator-independent
 framework for the analysis of systems of ODEs
 in the context of neuronal modeling and provided
 a reference implementation for the selection and
 generation of appropriate integration schemes as
 open source software. 1180

In this section we will summarize the restric-
 tions of our framework, discuss alternative ideas
 for the implementation and describe possible future
 additions. 1184

The framework we propose is currently limited to
 the analysis of equations for non-stochastic single
 compartmental integrate-and-fire neuron models
 The reason for this is that the analysis toolbox was
 developed in the context of the NESTML project
 in which we put our main focus on the class of
 neurons presently available in the NEST simulator
 The extension of the framework to other classes of
 neurons is one of our current research objectives. In
 particular, this work includes support for systems of
 stochastic ODEs. The symbolic analysis of neuron
 ODEs enables generation of the sophisticated C++
 neuron implementation that switches between im-
 plicit and explicit solvers at run-time of the neurons
 depending on the runtime performance of the par-
 ticular solver. This functionality will be integrated
 in upcoming releases of NESTML. 1201

Another restriction of the framework is that it can
 only analyze systems of ODEs with postsynaptic
 shapes that obey a linear homogeneous ODE. This
 is due to the fact that evolving a system including
 postsynaptic shapes as functions of time rather than
 functions defined as ODEs would result in a very
 long sum of multiple linear combinations of shifts
 of this function for each incoming spike. Evaluating
 such a sum would make the evolution of the system
 containing it computationally very costly. Finding a
 more efficient solution for this problem is of high
 priority in our current work. 1213

As noted in Section 2, the calculation of e^{Ah} may
 become difficult to compute analytically rather than
 numerically if the matrix A becomes very large. In

1217 this case, i.e. when e^{Ah} is computed as a numerical
 1218 approximation, the integration scheme is, strictly
 1219 speaking, not analytical. Here it might be sensible to
 1220 look into other numerical methods, e.g. integrating
 1221 the system of ODEs using a quadrature formula of
 1222 order 5 and thereby obtaining an accuracy of 10^{-8}
 1223 despite the use of a numerical scheme.

1224 When comparing implicit and explicit integration
 1225 schemes, we compare the *average step size* and the
 1226 *minimal step size* of the respective schemes. An
 1227 alternative possibility would be to use fixed step
 1228 sizes instead and compare the results of the explicit
 1229 and implicit schemes using the results of the implicit
 1230 scheme as a reference. This could be implemented
 1231 alongside our current stiffness tester to provide a
 1232 higher degree of certainty.

1233 As pointed out in Section 4, the stiffness of a
 1234 system of ODEs depends greatly on its parametriza-
 1235 tion. Therefore it might be a useful extension to
 1236 run the stiffness test not only during the generation
 1237 of the model code, but also when instantiating the
 1238 model in a simulator, and when model parameters
 1239 are changed. This would, however, require a call
 1240 to the analysis toolbox at run time, which might
 1241 not be easily possible on all machines a particular
 1242 simulator may run on. For example, in a supercom-
 1243 puter environment, job allocations are usually fixed,
 1244 and not all libraries required by the toolbox may
 1245 be available. An alternative solution to the problem
 1246 could be to run the stiffness test for varying param-
 1247 eters during the generation phase of the model. This
 1248 way the analysis toolbox could create a lookup table,
 1249 mapping parameter values to the most appropriate
 1250 integration scheme.

1251 Another possible extension of the current frame-
 1252 work could be to implement implicit and explicit
 1253 integration schemes for evolving the systems of
 1254 ODEs during the stiffness analysis, and thereby
 1255 gain independence of PyGSL, which can be chal-
 1256 lenging to install. These custom implementations
 1257 could be tailored to our specific requirements and
 1258 give us more control over the integration scheme
 1259 and the exact methodology for adaptive step size
 1260 control.

The current implementation of the framework
 only supports fixed thresholds for the detection
 of spikes and evaluates the spiking criterion on a
 fixed temporal grid. A part of our current work is to
 evaluate more realistic scenarios, such as adaptive
 thresholds or precise detection of spike times in be-
 tween the grid points. For a general discussion on
 the topic, see Hanuschkin et al. (2010). 1268

Our presented framework is re-usable indepen-
 dently of NESTML and NEST. The source code is
 available under the terms of the GNU General Pub-
 lic License version 2 or later on GitHub at <https://github.com/nest/ode-toolbox/> and we
 hope that the code can serve both as a useful
 tool for neuroscientists today, and as a basis for a
 future community effort in developing a simulator
 independent system for the analysis of neuronal
 model equations. 1278

CONFLICT OF INTEREST STATEMENT

The authors declare that the research was conducted
 in the absence of any commercial or financial re-
 lationships that could be construed as a potential
 conflict of interest. 1282

AUTHOR CONTRIBUTIONS

IB developed the mathematical derivations of the
 solver selection system and devised the algorithms
 The reference implementation was conceived and
 created by IB and DP. DP integrated the framework
 into the NESTML system. JME and AM supervised
 and guided the work. The article was written jointly
 by all authors. 1289

FUNDING

This work was supported by the JARA-HPC Seed
 Fund *NESTML - A modeling language for spiking
 neuron and synapse models for NEST* and the
Initiative and Networking Fund of the Helmholtz
 Association and the Helmholtz Portfolio Theme *Sim-
 ulation and Modeling for the Human Brain*. The
 current work on NESTML is partly funded by the 1296

1297 European Union's Horizon 2020 research and in-
1298 novation programme under grant agreement No.
1299 720270.

ACKNOWLEDGMENTS

1300 We gratefully acknowledge the fruitful discussions
1301 with the users of NESTML, who provided use cases
1302 and guided the work through their critical questions
1303 and thoughts. We would especially like to thank
1304 Arnold Reusken, Markus Diesmann, Hans Ekke-
1305 hard Plesser, Guido Trenscher, Bernhard Rumpe and
1306 Tanguy Fardet for their ongoing support and interest
1307 in the NESTML project.

REFERENCES

1308 Benker, H. (2016). *MATHEMATICA kom-*
1309 *pakt: Mathematische Problemlösungen für Inge-*
1310 *nieure, Mathematiker und Naturwissenschaftler*
1311 (Springer)
1312 Brette, R. and Gerstner, W. (2005). Adaptive ex-
1313 ponential integrate-and-fire model as an effective
1314 description of neuronal activity. *Journal of Neu-*
1315 *rophysiol* 94, 3637–3642. doi:10.1152/jn.00686.
1316 2005
1317 Carnevale, N. T. and Hines, M. L. (2006). *The NEU-*
1318 *RON Book* (New York, NY, USA: Cambridge
1319 University Press)
1320 Connors, B. W. and Gutnick, M. J. (1990). Intrinsic
1321 firing patterns of diverse neocortical neurons.
1322 *Trends in neurosciences* 13, 99–104
1323 Dahmen, W. and Reusken, A. (2005). *Numerik für*
1324 *Naturwissenschaftler* (Springer)
1325 Erdweg, S., van der Storm, T., Völter, M., Boersma,
1326 M., Bosman, R., Cook, W. R., et al. (2013). The
1327 state of the art in language workbenches. In
1328 *Software Language Engineering*, eds. M. Erwig,
1329 R. F. Paige, and E. Van Wyk (Cham: Springer
1330 International Publishing), 197–217
1331 FitzHugh, R. (1961). Impulses and physiological
1332 states in theoretical models of nerve membrane.
1333 *Biophysical J.*
1334 Gewaltig, M.-O. and Diesmann, M. (2007). NEST
1335 (NEural Simulation Tool). *Scholarpedia*

Goodman, D. and Brette, R. (2009). The Brian
simulator. *Frontiers in Neuroscience* 1337
Gough, B. (2009). *GNU scientific library reference*
manual (Network Theory Ltd.) 1339
Grönniger, H., Krahn, H., Rumpe, B., Schindler,
M., and Völkel, S. (2008). Monticore: a frame-
work for the development of textual domain-
specific languages. In *Companion of the 30th in-*
ternational conference on Software engineering
(ACM), 925–926 1345
Hanuschkin, A., Kunkel, S., Helias, M., Morri-
son, A., and Diesmann, M. (2010). A general
and efficient method for incorporating precise
spike times in globally time-driven simulations
In *Frontiers in Neuroinform.* doi:10.3389/fninf
2010.00113 1351
Hines, M. and Carnevale, N. (2000). Expand-
ing NEURON's repertoire of mechanisms with
NMODL. *Neural Computation* 1354
Izhikevich, E. M. (2003). Simple model of spiking
neurons. *IEEE Transactions on neural networks*
14, 1569–1572 1357
Kandel, E. R., Schwartz, J. H., Jessell, T. M., Siegel-
baum, S. A., and Hudspeth, A. (2013). *Principles*
of Neural Science. Principles of Neural Science
(McGraw-Hill Education), fifth edn. 1361
Krahn, H. (2010). *MontiCore: Agile Entwicklung*
von domänenspezifischen Sprachen im Software
Engineering. No. 1 in *Aachener Informatik*
Berichte, Software Engineering (Shaker Verlag) 1365
Krahn, H., Rumpe, B., and Völkel, S. (2007).
Efficient Editor Generation for Compositional
DSLs in Eclipse. In *Domain-Specific Model-*
ing Workshop (DSM'07) (Jyväskylä University
Finland) 1370
Kunkel, S., Diesmann, M., and Morrison, A. (2010).
Limits to the development of feed-forward struc-
tures in large recurrent neuronal networks. *Fron-*
tiers in Computational Neuroscience 4, 1–15
doi:10.3389/fncom.2010.00160 1375
Kunkel, S., Morrison, A., Weidel, P., Eppler, J. M.,
Sinha, A., Schenck, W., et al. (2017). NEST
2.12.0 1378
Kunkel, S., Schmidt, M., Eppler, J. M., Plesser,
H. E., Masumoto, G., Igarashi, J., et al. (2014)

- 1381 Spiking network simulation code for petascale
1382 computers. *Frontiers in Neuroinformatics* 8
- 1383 Lambert, J. D. (1992). *Numerical Methods for*
1384 *Ordinary Differential Systems* (Wiley)
- 1385 Meurer, A., Smith, C. P., Paprocki, M., Čertík,
1386 O., Kirpichev, S. B., Rocklin, M., et al. (2017).
1387 SymPy: symbolic computing in Python. *PeerJ*
1388 *Computer Science* 3, e103. doi:10.7717/peerj-cs.
1389 103
- 1390 Mir Seyed Nazari, P. (2017). *MontiCore: Effi-*
1391 *cient Development of Composed Modeling Lan-*
1392 *guage Essentials*. Aachener Informatik-Berichte,
1393 Software Engineering, Band 29 (Shaker Verlag)
- 1394 Morris, C. and Lecar, H. (1981). Voltage oscillations
1395 in the barnacle giant muscle fiber. *Biophys.*
1396 *J.*
- 1397 Morrison, A., Straube, S., Plesser, H. P., and Dies-
1398 mann, M. (2007). Exact Subthreshold Integration
1399 with Continuous Spike Times in Discrete-Time
1400 Neural Network Simulations. *Neural Computa-*
1401 *tion*
- 1402 Nagumo, J., Arimoto, S., and Yoshizawa, S. (1962).
1403 An active pulse transmission line simulating
1404 nerve axon. *Proc. IRE*.
- 1405 Pauli, R., Weidel, P., Kunkel, S., and Morrison, A.
1406 (2018). Reproducing polychronization: a guide
1407 to maximizing the reproducibility of spiking net-
1408 work models. *Frontiers in Neuroinformatics* (in
1409 press)
- 1410 Petzold, L. (1983). Automatic selection of methods
1411 for solving stiff and nonstiff systems of ordinary
1412 differential equations. *SIAM Journal on Scientific*
1413 *and Statistical Computing* 4, 136–148. doi:10.
1414 1137/0904010
- 1415 Plotnikov, D., Blundell, I., Ippen, T., Eppler, J. M.,
1416 Morrison, A., and Rumpe, B. (2016). NESTML:
1417 a modeling language for spiking neurons. In
1418 *Modellierung 2016 Conference* (Bonner Köllen
1419 Verlag), vol. 254 of *LNI*, 93–108
- 1420 Potjans, T. and Diesmann, M. (2012). The cell-type
1421 specific cortical microcircuit: relating structure
1422 and activity in a full-scale spiking network model.
1423 *Cerebral Cortex* 24
- 1424 Rotter, S. and Diesmann, M. (1999). Exact dig-
1425 ital simulation of time-invariant linear systems
with applications to neuronal modeling. *Bio-*
logical Cybernetics 81, 381–402. doi:10.1007/A427
s004220050570 1428
- Rumpe, B. (2017). *Agile Modeling with UML*
Code Generation, Testing, Refactoring (Springer)
International) 1431
- Schindler, M. (2012). *Eine Werkzeuginfrastruktur*
zur agilen Entwicklung mit der UML/P. Aach-
ener Informatik-Berichte, Software Engineering
Band 11 (Shaker Verlag) 1435
- Shampine, L. (1983). Type-insensitive ode codes
based on extrapolation methods. *SIAM Journal*
on Scientific and Statistical Computing 4, 635–
644. doi:10.1137/0904044 1439
- Shampine, L. (1991). Diagnosing stiffness for
Runge–Kutta methods. *SIAM Journal on Sci-*
entific and Statistical Computing 12, 260–272
doi:10.1137/0912015 1443
- Stimberg, M., Goodman, Benichoux, V., and Brette,
R. (2014). Equation-oriented specification of
neural models for simulations. *Frontiers in*
Neuroinformatics 1447
- Strehmel, K. and Weiner, R. (1995). *Nu-*
merik gewöhnlicher Differentialgleichungen
(B.G. Teubner) 1450
- Tiller, M. (2001). *Introduction to physical modeling*
with Modelica (Kluwer Academic Publishers) 1452
- van Albada, S. J., Helias, M., and Diesmann, M.
(2015). Scalability of asynchronous networks is
limited by one-to-one mapping between effective
connectivity and correlations. *PLOS Computa-*
tional Biology 11, 1–37. doi:10.1371/journal.
pcbi.1004490 1458
- Völkel, S. (2011). *Kompositionale Entwick-*
lung domänenspezifischer Sprachen. Aach-
ener Informatik-Berichte, Software Engineering
Band 9 (Shaker Verlag) 1462
- Walter, W. (2000). *Gewöhnliche Differentialgle-*
ichungen (Springer) 1464
- Westermann, T. (2010). *Mathematische Probleme*
lösen mit Maple (Springer) 1466